Pulse wave velocity measurement along the ulnar artery in the wrist region using a high frequency ultrasonic array

Maxime Benchemoul[1,2], Tony Matéo[1], David Savéry[1], Claudine Gehin[2], Bertrand Massot[2], Guillaume Ferin[1], Philippe Vince[1], Martin Flesch[1]

[1]*Active Probe Dpt., Vermon S.A.,* 37000 Tours, France
[2]*Univ. Lyon, INSA Lyon, ECL, CNRS, UCBL, CPE Lyon, INL, UMR5270,* 69621 Villeurbanne, France

Abstract—**A pulse wave velocity (PWV) measurement method performed above a small blood vessel using an ultrasonic probe is studied and reported in this paper. These experimentations are carried out using a high-frequency probe (14-22 MHz), allowing a high level of resolution compatible with the vessel dimensions, combined with an open research ultrasound scanner. High frame-rate (HFR) imaging (10 000 frames per second) is used for a precise PWV estimation. The measurements are performed in-vivo on a healthy volunteer. The probe is placed above the ulnar artery on the wrist in order to make longitudinal scans. In addition to conventional duplex ultrasound evaluation, the measurement of the PWV using this method at this location could strengthen the detection and diagnosis of cardiovascular diseases (CVDs), in particular for arm artery diseases (AADs). Moreover, these experimentations are also carried out within the scope of a demonstration for a potential miniaturized and wearable device (i.e., a probe with fewer elements, typically less than 32, and its associated electronics). The study has shown results coherent with expected PWV and also promising complementary results such as intima-media thickness (IMT) with spatiotemporal resolution on the order of 6.2 μm and 0.1 ms.**

Keywords—*Pulse wave velocity, intima-media thickness, cardiovascular diseases, arm artery disease, ultrasounds, ulnar artery, wall detection, non-invasive, ultra-fast imaging.*

I. INTRODUCTION

Cardio-vascular diseases are the major death causes as they represent more than one third of casualties all around the world according to the World Health Organization [1]. Their prevention by early detection and monitoring is an important concern and requires specific and simple to use tools. The PWV is likely to detect premises of CVD or AAD since it directly reflects the age and health of the arterial network. This has been strongly investigated and demonstrated by a wide range of studies in the past decades [2] [3] [4].

In each cardiac cycle, the heart pumps blood which generates a pressure wave. The resulting pulse wave propagates all along the arterial tree which slightly deforms the arteries wall, the blood being a quasi-incompressible fluid. The stiffness of the artery naturally increases with age and so does the PWV: indeed, the stiffer the arteries are, the higher the PWV is. However, this phenomenon can be accentuated when atherosclerosis appears [5] – this disease results in the formation of atheromatous plaques caused by lipid retention. At an early stage of the disease, there are no particular symptoms – it goes silent and progressive from potentially young age to middle age. Later, depending on the

severity of the symptoms, it can lead to serious diseases (cerebrovascular accident, myocardial infarction, coronary or peripheral artery disease) [6]. Hence, a reliable, non-invasive, cost-effective and easy method would be a great asset for periodical routine check-ups to detect as early as possible this kind of pathology. In this context, we present through this work the development and feasibility of an ultrasonic method to assess local PWV on the wrist above the ulnar artery using a high frequency probe allowing both wall motion detection and artery anatomy study. The structure of the paper is organized as follows: Section II presents the pulsatile flow mechanism. Then the material and methods Section III describes the measurement method, the probe used during the experiments, the ultrasound scanner setup as well as the algorithm applied to extract the PWV from the ultrasonic data. Finally, the results and the analysis of the experimental measurements are reported in Section IV.

II. PULSATILE FLOW AND PRESSURE WAVE

At the beginning of the cardiac cycle, the contraction of the left ventricle generates a flow gradient which is characterized by a pressure gradient since the arteries have viscoelastic properties. Navier-Stokes equations describe this pulsatile blood flow behavior [7] [8]:

$$-\frac{dP}{dx} = \rho\left(\frac{dv}{dt} + u\frac{dv}{dr} + v\frac{dv}{dx}\right) - \mu\left(\frac{d^2v}{dr^2} + \frac{1}{r}\frac{dv}{dr} + \frac{d^2v}{dx^2}\right) \quad (1)$$

$$-\frac{dP}{dr} = \rho\left(\frac{du}{dt} + u\frac{du}{dr} + v\frac{du}{dx}\right) - \mu\left(\frac{d^2u}{dr^2} + \frac{1}{r}\frac{du}{dr} + \frac{d^2u}{dx^2} - \frac{u}{r^2}\right) (2)$$

where dP is described as longitudinal (dx) and radial (dr) pressure gradient. The parameters u and v represent respectively the longitudinal and radial blood velocity. The parameter ρ designates the density of the blood and μ its viscosity. By simplification of the Navier-Stokes equation (1) (non-linear terms and viscous drag are neglected), we deduce the following relation along the x-axis:

$$-\frac{dP}{dx} = \rho\frac{dv}{dt} = \frac{\rho}{\bar{A}}\frac{\bar{A}dv}{dt} = \frac{\rho}{\bar{A}}\frac{dQ}{dt} \quad (3)$$

where $\bar{A}$ is the time-averaged cross-section area and Q is the volumetric flow. In fact, the viscous drag along the artery tends to attenuate the pulse wave amplitude. Assuming that blood is a Newtonian fluid, the consequence of the generated flow gradient is a change in the cross section:

$$-\frac{dQ}{dx} = \frac{dA}{dt} = \frac{dA}{dP}\frac{dP}{dt} \quad (4)$$

The pressure wave (variable over time) propagates along the artery generating a flow gradient and thus a local rise of the pressure and the section (artery dilation). This phenomenon is called pulse wave and its velocity (PWV) is given by the Bramwell-Hill [9] equation:

$$PWV_{BH} = \sqrt{\frac{\overline{A}}{\rho} \frac{dP}{dA}} \qquad (5)$$

Moreover, the other PWV equation by Moens-Korteweg [10] describes the physical properties of the artery:

$$PWV_{MK} = \sqrt{\frac{Eh}{2\rho R(1 - v^2)}} \qquad (6)$$

where h is the wall thickness, ρ is the density of blood, R is the radius of the artery, E is the Young's modulus of the artery wall and v its Poisson's ratio. This rapid demonstration makes it easy to see how atherosclerosis can affect PWV by reducing locally the size of an artery and also how premature aging of the arterial tree can affect PWV. It clearly proves that PWV is one of the most relevant cardiovascular parameters for the detection and monitoring of CVDs. The strength of an ultrasound method compared to other modalities is not only to characterize a pulse wave by detecting an artery wall motion but also to precisely measure the physical dimensions of an artery, such as its diameter or its wall thickness dynamically during the pulse wave propagation.

III. MATERIAL AND METHODS

A. PWV measurement method

There are three kinds of PWV measurements: local, peripheral and central. Most of the time, peripheral and central measurements are made using two synchronized applanation tonometers (pressure sensors) at two separate measurement sites (respectively carotid-radial, and carotid-femoral). This technique is also known as the pulse transit time (PTT) method. The mean velocity along the arterial path is calculated using the measured transit time between the two pressure curves and an approximative distance between the two measurement sites. Applanation tonometry is considered as the gold-standard for PWV assessment. These conventional central and peripheral measurements are widely used and have demonstrated through many studies the significance of PWV to assess and detect cardiovascular anomalies [2] [11].

However, there are emerging techniques using other sensing modalities. Most of them use PTT methods to calculate the PWV. Among them we can mention:

- Photoplethysmography (PPG) combined with synchronized electrocardiography (ECG) [12] for peripheral PWV,

- Applanation tonometry synchronized with an ECG [13] for peripheral PWV,

- Dual synchronized PPG sensors [14] for central, local or peripheral PWV,

- Ballistocardiography synchronized with impedance plethysmography [15] for central PWV.

In addition to these various techniques, we also find ultrasonic measurements of the PWV which are made using PTT measurements [16] or Doppler derived methods such as flow-section analysis [8] [17], pulsed Doppler synchronized with an ECG [18] or dual pulsed Doppler [19], that have been clinically tested.

One of the main advantages of the ultrasonic techniques is the capacity to perform not only peripheral and central measurements but also local measurements. Two examples of local PWV methods are presented in Figure 1. This is made possible by the arrival in the last decade of ultrafast imaging allowing very high frame-rates (> 1000 frames/s) and thus to detect fast transient motion of the tissues. Unlike the peripheral and central PWV measurements, it allows accurate quantification of the PWV along the targeted artery and provides better information about its biomechanical properties (and eventually abnormalities) [20]. The other advantage is that only a single and conventional ultrasonic probe apparatus is needed to perform such measurements.
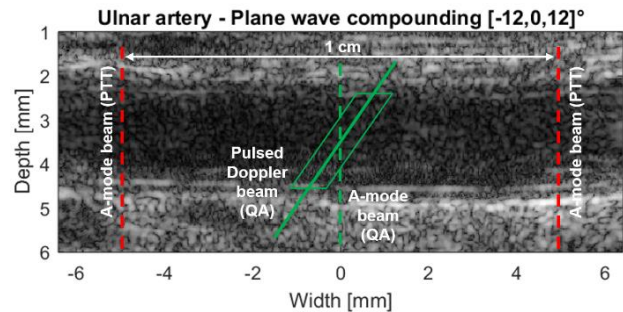

Figure 1: Principles of local PWV measurement methods on a longitudinal artery ultrasonic scan. In red, two A-mode RF-lines are used to measure the pulse transit time (PTT method). In green, one A-mode line measures the diameter of the artery over time and a pulsed Doppler sequence measures the blood flow in order to plot the flow-section curve (QA method).

In the experimentation proposed here, the PWV is calculated using radiofrequency (RF) raw ultrasonic data from a longitudinal scan of the ulnar artery. Two axial reconstructed lines, separated by 1 cm on the x-axis as shown in red dotted lines on Figure 1, are post-processed to extract the artery diameter. Then the transit time of the local pulse wave is calculated from the time-delay of the two resulting curves. All of this using only a few elements of the probe to stay compatible with the idea of integrating a miniaturized probe and system within a wearable device.

B. High-frequency ultrasonic probe

The ultrasonic probe used here is a high-frequency (HF) linear array (L22-14v) manufactured by Vermon S.A. (Tours, France), whose acoustic and geometric parameters are suited to high-resolution imaging of superficial structures. The main specifications are the following:

- Single crystal transducer,
- 18.5 MHz center frequency (f_c),
- Relative transmit-receive bandwidth (-6 dB) of 70%,
- 128 elements,
- 100 µm pitch,

- 8 mm elevation focus.

Considering the anatomy of the wrist around the ulnar artery and its size (~ 2.4 mm diameter, 3 to 5 mm depth), a high-frequency probe is required to keep a good axial resolution for a precise diameter measurement. The optimum axial resolution is defined by half of the ultrasonic transmit frequency wavelength λ. Here it corresponds to 42 µm at 18.5 MHz or 50 µm at 15.625 MHz.

C. Verasonics Vantage-256™ HF: open research scanner

The probe is connected to an open US scanner Verasonics Vantage-256™ HF (see Figure 2). It uses custom scripts handling high frame-rate coherent plane-wave compounding based on Verasonics HFR acquire and reconstruction scripts. The main parameters of the US sequence are the following:

- Emitting frequency (f_e) = 15.625 MHz
- Transmit excitation duration = 1 half cycle
- Transmit voltage = 25 V
- Analog-to-digital (ADC) sampling rate = 62.5 MSPS
- Flat plane-wave with 0° transmit angle
- Frame-rate (f_r) = 10 kHz
- Total imaging depth = 1 to 6 mm

In order to get the best spatial resolution, compliant with the maximum Vantage's ADC sampling rate (62.5 MHz), the transmit frequency has been fixed to 15.625 MHz which is still inside the bandwidth of the transducer (λ = 50 µm).
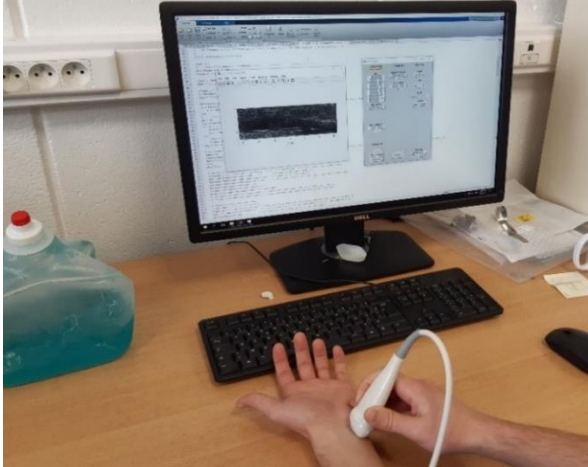

Figure 2: Experimental setup using a Verasonics Vantage™ and a high frequency linear array L22-14v

D. Wall-motion and PWV calculation algorithm

The typical received beamformed image has a frame-size of 812 by 128 pixels, which corresponds to a reconstructed axial resolution of λ/16 and lateral resolution of λ, and 15 000 frames (i.e., sampled at 10 kHz during 1.5 second). For the wall-motion tracking algorithm, two axial scan lines, $A(k)$ and $B(k)$ (envelop of RF scan lines) spaced by 1 cm (~ 100 λ) are extracted from the dataset and 2D spline interpolation is processed to enhance their axial (×16) and temporal (×4) resolutions, in regards to the low artery expansion (between λ and 2λ) and the expected fast pulse propagation (~1 ms delay for 1 cm distance). Then, a basic wall motion tracking algorithm is applied to each of the resulting lines: the initial tracking points are manually

selected (inner and outer layer of the vessel walls) and the algorithm tracks the position of the corresponding envelop peaks through the 4×15 000 samples using a simple max function. The resulting tracked points are shown in the following section on Figure 4.
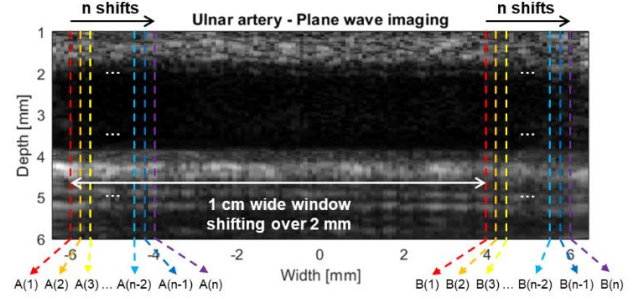

Figure 3: B-mode longitudinal image of the ulnar artery near the wrist with a graphic representation of the 1 cm wide shifting window made of several pairs of scan lines [A(k), B(k)]

The two diameter curves are filtered using a smoothing low-pass filter and the regions corresponding to the cardiac cycles are manually isolated. A cross-correlation between the two curves is computed. This process is repeated using a lateral shifting window over 2 mm ($n = 11$), as shown on Figure 3, using only a few elements of the probe and therefore reducing data and computing time. All the cross-correlation results are finally averaged to calculate the mean cross-correlation. The interpolated time shift that maximizes the average cross-correlation gives the mean time-shift between pairs of scan lines separated by a fixed distance. The mean PWV (m/s) is calculated using the following formula:

$$\overline{PWV_{PTT}} = \frac{I_R f_r \Delta d}{\bar{\delta}} \qquad (7)$$

Where I_R is the temporal interpolation factor, f_r (Hz) the frame-rate, Δd (m) the fixed distance between each pair of scan lines and $\bar{\delta}$ the maximizing interpolated time shift, in number of frames, between the two cardiac cycles curves.

IV. RESULTS AND DISCUSSION

A. Visualization of the phenomenon

A simple way to observe the pulse wave phenomenon and the induced artery dilation is to display the envelop of a scan
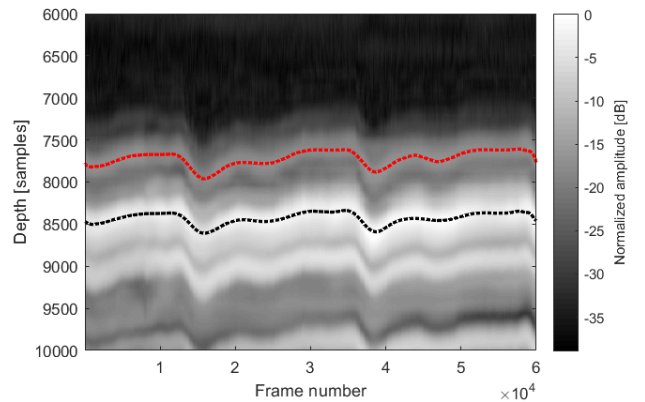

Figure 4: M-mode imaging of a scan line at -5 mm on the width axis, zoomed on the posterior wall (corresponding depth range: 3.31 mm to 4.85 mm)

line through time: this kind of representation corresponds to M-mode ultrasound imaging. It is often used in echocardiography imaging because of its very good temporal resolution allowing the recording of structures moving at high velocities as fetal heart beats. Here, combined with a very good axial resolution, M-mode imaging has been used in a first approach to analyze the displacement of the artery walls during the propagation of the pulse wave. An extract of the M-mode image made from a scan line clearly shows, in Figure 4, the posterior wall displacement over time. Reflected echoes from the inner and outer layers of the artery wall have been tracked by the wall motion algorithm. They are respectively denoted by the upper red dotted line and the lower black dotted line.

B. Analysis and PWV calculation

A lot of information can be extracted from the different measured curves of the artery walls. The major one is the artery diameter at two different sites as shown on Figure 6. As explained earlier, this measurement is realized on a shifting window over 2 mm and the mean cross-correlation gives the mean shift between the two diameter curves. Here with the presented dataset, 9 of the 11 cross-correlated results have been kept after data cleaning (i.e., curves with non-representative shapes due to wall motion tracking failures have been removed). The calculated average artery diameter is 2.61 mm and the average variation in diameter is 4.6 %. A mean shift of 48.5 samples has been extracted from the average cross-correlation, resulting in an average PWV of 8.25 m/s over 2 cardiac cycles.
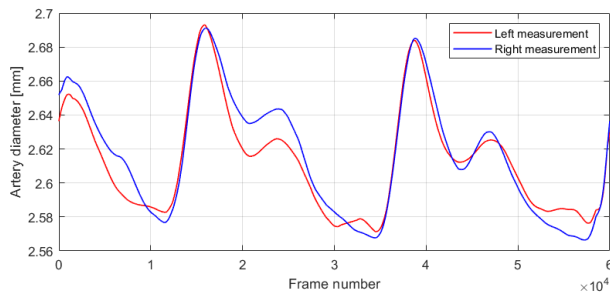

Figure 6: Pair of artery diameter measurements spaced 1 cm apart along the ulnar artery

Regarding the Bramwell-Hill (5) and Moens-Korteweg (6) equations as well as typical PWV values on larger arteries (between 4 and 8 m/s for the carotid artery [21] [22]) and similar small arteries (between 7 and 9 m/s for the radial artery [23] or brachial-radial arteries [24]) this calculated value is coherent.

Another interesting observation can be made when observing the intima-media thickness (ITM) evolution through time, obtained by calculating the difference between the tracked inner and outer layers of the artery wall as shown in Figure 4. The IMT curve, graphically illustrated in Figure 5, is quite noisy as it would require a higher axial resolution to gain accuracy. However, a closer view during the cardiac cycle shows a significant change of thickness at the systolic and diastolic peaks. The mean thickness of the IMT is 0.273 mm and its total variation is 38 µm over 2 cardiac cycles (as a reminder, axial resolution before interpolation is

6.16 µm). Knowing the mean IMT, the diameter or the artery and the blood velocity already makes possible to estimate the Young's modulus of the arterial wall. However, these data with improved spatiotemporal resolution could allow a better understanding of the biomechanical behavior of the artery and a better estimation of the arterial stiffness.
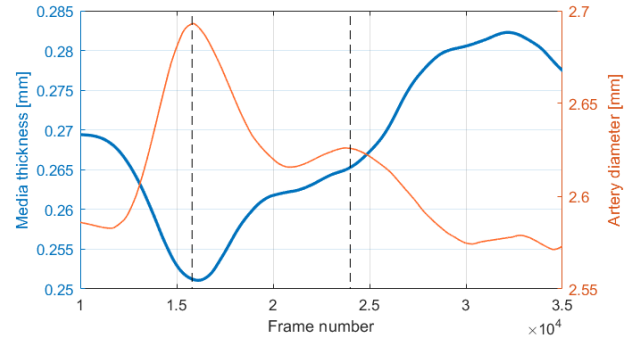

Figure 5: Visualization of the IMT (blue) during the cardiac cycle in regards to the artery diameter curve (red)

V. CONCLUSION & PERSPECTIVES

Studies have been carried on with a linear ultrasonic probe (15.625 MHz emitting frequency) and a high-frequency Verasonics Vantage scanner to realize an in-vivo proof-of-concept of the pulse wave visualization and velocity measurement. However, the propagating pulse wave and the associated pressure gradient only induce a slight dilation of the small peripheral ulnar artery. This makes the measurement using ultrasound imaging quite delicate and requires very high axial and temporal resolution. PTT method has been enhanced here to strengthen the transit time measurement but it might not be the best method to assess PWV at this location. Indeed, computing resources are still quite high (10 kHz frame rate combined with high axial resolution) and the wall tracking algorithm still need to be improved to make it more robust and fully automated. Preliminary results are nonetheless coherent with the expected range of PWV and other promising data have been observed, such as IMT with a great spatiotemporal resolution. These results have confirmed the possibility to measure low dilations on the ulnar artery and to extract the local PWV from the post-processed data using only two small acoustic apertures of the probe of 11 elements each. Thus, it makes these experimentations encouraging and promising in regards to our miniaturization and integration short-term objectives.

In the future, the usage of a calibration process will be considered with, for example, a pair of applanation tonometers placed at each side of the forearm along the ulnar artery in order to characterize reference PWV values. In addition, phantom in vitro experimentations will be carried out to enhance repeatability and wall motion tracking algorithm.

VI. REFERENCES

[1] "World Health Organization," 17 05 2017. [Online]. Available: https://www.who.int/en/news-room/fact-

sheets/detail/cardiovascular-diseases-(cvds). [Accessed 18 01 2021].

[2] L. HS and L. GYH, "Arterial stiffness: beyond pulse wave velocity and its measurement," *Journal of Human Hypertension,* vol. 22, pp. 656-658, 2008.

[3] P. Boutouyrie, M. Briet, C. Collin, S. Vermeersch and B. Pannier, "Assessment of pulse wave velocity," *Artery Research,* vol. 3, pp. 3-8, 2009.

[4] A. R. Khoshdel, S. L. Carney, B. R. Nair and A. Gillies, "Better management of cardiovascular diseases by pulse wave velocity: combining clinical practice with clinical research using evidence-based medicine," *Clinical Medicine & Research,* vol. 5, pp. 45-52, 2007.

[5] K. Kobayashi, M. Akishita, W. Yu, M. Hashimoto, M. Ohni and K. Toba, "Interrelationship between non-invasive measurements of atherosclerosis: flow-mediated dilation of brachial artery, carotid intima-media thickness and pulse wave velocity," *Atherosclerosis,* vol. 173, pp. 13-18, 2004.

[6] R. Ross, "Atherosclerosis - an inflammatory disease," *The New England Journal of Medicine,* vol. 340, pp. 115-126, 1999.

[7] W. R. Wilnor, Hemodynamics, Baltimore: William & Wilkins, 1989.

[8] J. Seo, *Continuous and Non-invasive Blood Pressure Monitoring using Ultrasonic Methods,* MIT thesis, 2014.

[9] J. C. Bramwell and A. V. Hill, "The velocity of pulse wave in man," *Royal Society,* vol. 93, 1922.

[10] A. S. Tijsseling and A. Anderson, "A. Isebree Moens and D.J. Korteweg: on the speed of propagation of waves in elastic tubes," *International Conference on Pressure Surges (Conf. paper),* pp. 227-245, 2012.

[11] A. P. Avolio, M. Butlin and A. Walsh, "Arterial blood pressure measurement and pulse wave analysis- their role in enchancing cardiovascular assessment," *Physiological Measurement,* vol. 31, pp. 1-47, 2010.

[12] S. Loukogeorgakis, R. Dawson, N. Phillips, C. N. Martyn and S. E. Greenwald, "Validation of a device to measure arterial pulse wave velocity by a photoplethysmographic method," *Physiological Measurement,* vol. 23, pp. 581-596, 2002.

[13] P. Salvi, G. Lio, C. Labat, E. Ricci, B. Pannier and A. Benetos, "Validation of a new non-invasive portable tonometer for determining arterial pressure wave and pulse wave velocity: the PulsePen device," *Journal of Hypertension,* vol. 22, pp. 2285-2293, 2004.

[14] N. P.M., J. Joseph, V. Awasthi and M. Sivaprakasam, "Single source photoplethysmograph transducer for local pulse wave velocity measurement," *Engineering in Medicine and Biology Society,* 2016.

[15] D. Campo, H. Khettab, R. Yu, N. Genain, P. Edouard, N. Buard and P. Boutouyrie, "Measurement of aortic pulse wave velocity with a connected bathroom scale," *American Journal of Hypertension,* vol. 30, pp. 876-883, 2017.

[16] C.-C. Huang, H.-F. Cheng, B.-P. Zhu, P.-Y. Chen, S. T. Beh, Y.-M. Kuo and C.-C. Huang, "Studying arterial stiffness using high-frequency ultrasound in mice with Alzheimer disease," *Ultrasound in Medicine and Biology,* vol. 43, no. 9, pp. 1-11, 2017.

[17] R. Williams, A. Needles, E. Cherin, Y.-Q. Zhou, R. M. Henkelman, S. L. Adamson and F. S. Foster, "Noninvasive ultrasonic measurement of regional and local pulse-wave velocity in mice," *Ultrasound in Medicine and Biology,* vol. 33, no. 9, pp. 1368-1375, 2007.

[18] B. Jiang, B. Liu, K. L. Mcneill and P. J. Chowienczyk, "Measurement of pulse wave velocity using pulse wave Doppler ultrasound: comparison with arterial tonometry," *Ultrasound in Medicine & Biology,* vol. 34, pp. 209-512, 2008.

[19] Z. Wang, Y. Y. L.-j. Yang, J. Liu, Y.-y. Duan and T.-s. Cao, "Noninvasive method for measuring local pulse wave velocity by dual pulse wave Doppler: in-vitro and in-vivo studies," *Plos ONE,* vol. 10, 2015.

[20] T. Pereira, C. Correia and J. Cardoso, "Novel methods for pulse wave velocity measurements," *Journal of Medical and Biomedical Engineering,* vol. 35, pp. 555-565, 2015.

[21] C.-J. Tang, P.-Y. Lee, Y.-H. Chuang and C.-C. Huang, "Measurement of local pulse wave velocity for carotid artery by using an ultrasound-based method," *Ultrasonics,* vol. 102, 2020.

[22] H. Hasegawa, K. Hongo and K. Hiroshi, "Measurement of regional pulse wave velocity using very high frame rate ultrasound," *Journal of Medical Ultrasonics,* vol. 40, no. 2, pp. 91-98, 2013.

[23] Y.-L. Zhang, Z.-C. Ma, C.-W. Lung, Y.-N. Sun and X.-H. Li, "A new approach for assessment of pulse wave velocity at radial artery in young and middle-aged healthy humans," *Journal of Mechanics in Medicine and Biology,* vol. 12, 2012.

[24] N. Cauwenberghs, Y. Heyrman, L. Thijs, W.-Y. Yang, F.-F. Wei, Z.-Y. Zhang, J. A. Staessen and T. Kuznetsova, "Flow-mediated slowing of brachial-radial pulse wave velocity: methodological aspects and clinical determinants," *Artery Research,* vol. 21, pp. 29-37, 2018.